Chemistry of Metals and Alloys

Chem. Met. Alloys 9 (2016) 72-77
Ivan Franko National University of Lviv
www.chemetal-journal.org

Contribution to the investigation of the Sm–Cu–Sn ternary system

L. ROMAKA[1]*, V.V. ROMAKA[2], A. HORYN[1], Yu. STADNYK[1]

[1] *Department of Inorganic Chemistry, Ivan Franko National University of Lviv, Kyryla i Mefodiya St. 6, 79005 Lviv, Ukraine*
[2] *Department of Materials Engineering and Applied Physics, Lviv Polytechnic National University, Ustyyanovycha St. 5, 79013, Lviv, Ukraine*
* *Corresponding author. E-mail: romakal@lnu.edu.ua*

Received June 16, 2016; accepted June 29, 2016; available on-line November 7, 2016

The isothermal section of the phase diagram of the Sm–Cu–Sn ternary system was constructed at 870 K in the whole concentration range based on X-ray diffraction and EPM analysis. The interaction between the elements results in the formation of five ternary compounds at this temperature: SmCuSn (NdPtSb-type), $Sm_3Cu_4Sn_4$ ($Gd_3Cu_4Ge_4$-type), $SmCu_5Sn$ ($CeCu_5Au$-type), $Sm_{1.9}Cu_{9.2}Sn_{2.8}$ (related to $CeNi_5Sn$-type), and $SmCu_2Sn_2$ ($CaBe_2Ge_2$-type). DSC analyses showed a limited stability range for the $Sm_2Cu_4Sn_5$ compound (up to 811 K), as well as for the isotypic $R_2Cu_{4-x}Sn_{5+x}$ compounds with Pr (496-783 K) and Nd (671-791 K). Rietveld refinement of the crystal structure of $SmCu_5Sn$ confirmed $CeCu_5Au$-type atom ordering (space group *Pnma*, *a* = 0.8267(1), *b* = 0.50087(6), *c* = 1.0601(1) nm).

Intermetallics / Phase diagrams / X-ray diffraction / Rare earth metal system

1. Introduction

Investigation of the phase equilibria in metallic systems by constructing isothermal sections at selected temperatures provides information on the formation, stability, and homogeneity range of the intermetallic compounds, and the heat treatments necessary to obtain homogenous samples. Because of the low melting temperature of Sn, most of the *R*–Cu–Sn systems have been studied at 670 K [1-6]. Recently, we studied the interactions of the component in the Dy–Cu–Sn and Gd–Cu–Sn ternary systems at 670 and 770 K and analyzed the influence of the heat treatment on the stability of the formed compounds [7,8]. The most remarkable difference between the two temperatures concerned the $R_2Cu_{4-x}Sn_{5+x}$ phases ($Sm_2Cu_4Sn_5$-type, space group *I*4*mm*), which were found to exist at 670 K, while at 770 K they were not observed [9]. DSC analysis confirmed the limited temperature range of the compounds with Sn content higher than 50 at.% in the {Gd, Tb, Dy}–Cu–Sn systems. This observation is in a good agreement with the binary Cu–Sn system [10], which is characterized by low temperatures of formation of the binary phases in the region with more than 50 at.% Sn, and by the presence of a broad liquid range down to low temperature. The influence of the temperature on the crystal structure of the $R_3Cu_4Sn_4$ compounds (*R* = Tm, Lu), characterized by two structural (monoclinic $Tm_3Cu_4Sn_4$-type and orthorhombic $Gd_3Cu_4Ge_4$-type) modifications, was studied in [11].

The phase diagram of the Sm–Cu–Sn ternary system at 770 K was reported in [5]; seven ternary compounds were observed at the temperature of investigation. The structures of the phases of approximate compositions ~$Sm_{15}Cu_{65}Sn_{20}$ and ~$Sm_{44}Cu_{35}Sn_{21}$ were not determined. The crystal structure of $Sm_{1.9}Cu_{9.2}Sn_{2.8}$ was reported a few years later [12].

In the present work the phase equilibria in the Sm–Cu–Sn system at 870 K were studied by X-ray diffraction and EPM analysis and the influence of the heat treatment on the stability of the ternary $R_2Cu_{4-x}Sn_{5+x}$ phases with Pr, Nd, and Sm was analyzed by DSC. The data concerning the Sm–Sn, Sm–Cu and Cu–Sn binary systems were taken from [10,13-15].

2. Experimental details

The samples were prepared by direct two-fold arc melting of the constituent elements (rare earth, purity

99.9 wt.%; copper, purity 99.99 wt.%; and tin, purity 99.999 wt.%) under high-purity Ti-gettered argon atmosphere on a water-cooled copper crucible. The weight losses of the initial total mass were less than 1 wt.%. Pieces of the as-cast buttons were annealed for one month at 870 K in evacuated silica tubes and then water-quenched. Phase analysis was performed using X-ray powder diffraction diagrams of the samples (DRON-4.0, Fe K_α radiation). The observed diffraction intensities were compared with reference powder patterns of the binary and known ternary phases. The compositions of the samples were examined by scanning electron microscopy (SEM), using a REMMA-102-02 scanning microscope. Quantitative electron probe microanalysis (EPMA) was carried out with an energy-dispersive X-ray analyzer, using the pure elements as standards (the acceleration voltage was 20 kV; *K*- and *L*-lines were used). The crystallographic parameters and theoretical diffraction patterns were calculated using the WinCSD program package [16]. Rietveld refinements were performed using the WinPLOTR program package [17].

DSC analysis (LINSEIS STA PT 1600 device) was performed on the $R_2Cu_{4-x}Sn_{5+x}$ compounds (R = Pr, Nd, Sm) to check the limits of the stability ranges in temperature. The samples were heated in argon atmosphere up to 850 K at a rate of 10 K/min. The weight losses during heating (TG) were negligible (less than 0.3 %).

3. Results and discussion

The phase equilibria in the Sm–Cu–Sn phase diagram were investigated at 870 K based on X-ray diffraction and metallographic analysis of 17 binary and 33 ternary alloys. The isothermal section of the Sm–Cu–Sn ternary system at 870 K is presented in Fig. 1. The phase compositions of selected samples are listed in Table 1 and microphotographs are shown in Fig. 2.

To check the literature data on the binary boundary systems of the Sm–Cu–Sn system, all known binary compounds in the Sm–Cu and Cu–Sn systems were synthesized and confirmed in the course of our investigations (Fig. 1). In the Sm–Sn binary system the compounds $SmSn_3$, Sm_2Sn_5, Sm_3Sn_7, $SmSn_2$, Sm_5Sn_4, Sm_4Sn_3, and Sm_5Sn_3 were successfully obtained. To check the existence of the binary stannide Sm_2Sn_3 [15], a sample of composition $Sm_{40}Sn_{60}$ was prepared and annealed at 670 and 870 K. Phase analysis of the sample showed the presence of two phases, Sm_5Sn_4 and $SmSn_2$, at both temperatures.

The interaction of the components in the Sm–Cu–Sn system under the conditions applied here led to the formation of five ternary compounds: SmCuSn, $Sm_3Cu_4Sn_4$, $SmCu_5Sn$, $Sm_{1.9}Cu_{9.2}Sn_{2.8}$, and $SmCu_2Sn_2$, the crystallographic characteristics of which are listed in Table 2. All the ternary compounds in the Sm–Cu–Sn ternary system are characterized by

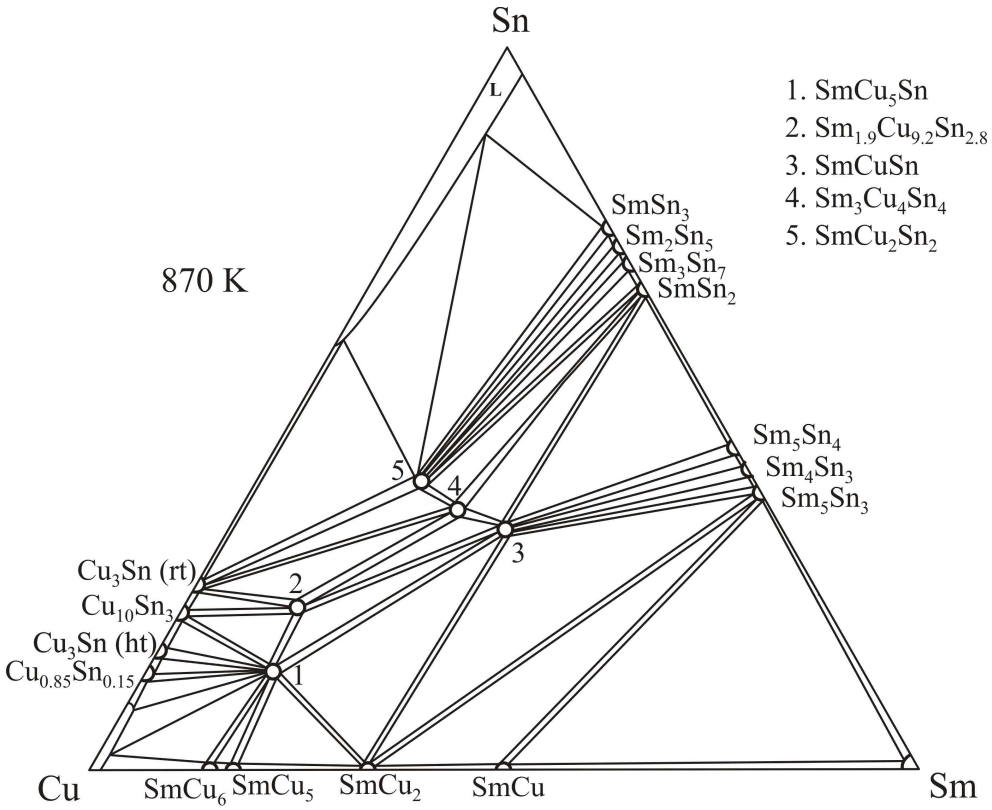

Fig. 1 Isothermal section of the Sm–Cu–Sn system at 870 K.

Table 1 Phase composition of selected Sm–Cu–Sn alloys.

No.	Nominal composition ot the alloy (at.%)			Phases		
	Sm	Cu	Sn	1st phase	2nd phase	3rd phase
1	17	73	10	$SmCu_5Sn$ *a* = 0.4984(4) nm *b* = 0.8263(4) nm *c* = 1.0540(6) nm	$SmCu_5$ *a* = 0.5072(4) nm *c* = 0.4097(8) nm	
2	15	70	15	$SmCu_5Sn$ *a* = 0.4985(4) nm *b* = 0.8262(4) nm *c* = 1.0542(6) nm	$Sm_{1.9}Cu_{9.2}Sn_{2.8}$ *a* = 0.5041(4) nm *c* = 2.0430(7) nm	
3	25	60	15	$SmCu_5Sn$ *a* = 0.4983(4) nm *b* = 0.8263(3) nm *c* = 1.0541(5) nm	SmCuSn *a* = 0.4547(3) nm *c* = 0.7477(4) nm	$SmCu_2$ (traces)
4	50	35	15	Sm_5Sn_3 *a* = 0.9090(4) nm *c* = 0.6611(4) nm	$SmCu_2$ *a* = 0.4357(3) nm *b* = 0.6927(4) nm *c* = 0.7377(8) nm	SmCu *a* = 0.3533(3) nm
5	20	60	20	$Sm_{1.9}Cu_{9.2}Sn_{2.8}$ *a* = 0.5044(3) nm *c* = 2.0428(9) nm	SmCuSn *a* = 0.4546(1) nm *c* = 0.7465(5) nm	$SmCu_5Sn$ *a* = 0.4980(6) nm *b* = 0.8260(3) nm *c* = 1.0544(7) nm
6	45	35	20	SmCuSn *a* = 0.4548(3) nm *c* = 0.7473(4) nm	Sm_5Sn_3 *a* = 0.9081(4) nm *c* = 0.6619(4) nm	$SmCu_2$ (traces)
7	15	60	25	$Sm_{1.9}Cu_{9.2}Sn_{2.8}$ *a* = 0.5046(3) nm *c* = 2.0425(7) nm	$Sm_3Cu_4Sn_4$ *a* = 0.4507(4) nm *b* = 0.6958(4) nm *c* = 1.4825(7) nm	Cu_3Sn *a* = 0.4321(4) nm *b* = 0.5486(5) nm *c* = 0.4739(4) nm
8	40	30	30	SmCuSn *a* = 0.4551(3) nm *c* = 0.7475(5) nm	Sm_5Sn_3 *a* = 0.9088(4) nm *c* = 0.6609(6) nm	$SmCu_2$ *a* = 0.4358(4) nm *b* = 0.6929(5) nm *c* = 0.7379(8) nm
9	23	40	37	$Sm_3Cu_4Sn_4$ *a* = 0.4506(3) nm *b* = 0.6960(3) nm *c* = 1.4824(6) nm	$SmCu_2Sn_2$ *a* = 0.4400(3) nm *c* = 1.0096(7) nm	
10	15	45	40	$SmCu_2Sn_2$ *a* = 0.4396(3) nm *c* = 1.0093(4) nm	Cu_3Sn *a* = 0.4319(3) nm *b* = 0.5488(4) nm *c* = 0.4737(4) nm	Sn *a* = 0.5807(2) nm *c* = 0.3177(3) nm
11	20	30	50	$SmCu_2Sn_2$ *a* = 0.4395(4) nm *c* = 1.0091(6) nm	$SmSn_3$ *a* = 0.4676(3) nm	Sn (traces)
12	30	20	50	$Sm_3Cu_4Sn_4$ *a* = 0.4509(3) nm *b* = 0.6961(4) nm *c* = 1.4822(8) nm	$SmSn_2$ *a* = 0.4419(4) nm *b* = 1.5837(6) nm *c* = 0.4501(3) nm	

a narrow homogeneity range at the temperature of investigation. The solubility of the third component in the binary phases was found to be less than 1-2 at.%.

To check the existence of the ternary compound at the composition ~$Sm_{44}Cu_{35}Sn_{21}$, reported earlier as a new ternary phase [6], samples near this composition were prepared and annealed at 770 and 870 K. Detailed phase analysis of the samples revealed that they belong to the three-phase field involving the main ternary phase SmCuSn with NdPtSb-type structure, in equilibrium with the binary phases Sm_5Sn_3 and $SmCu_2$ (Fig. 2a).

Previous investigations of the Cu-rich corner of the *R*–Cu–Sn ternary systems, where *R* = Y, La-Sm,

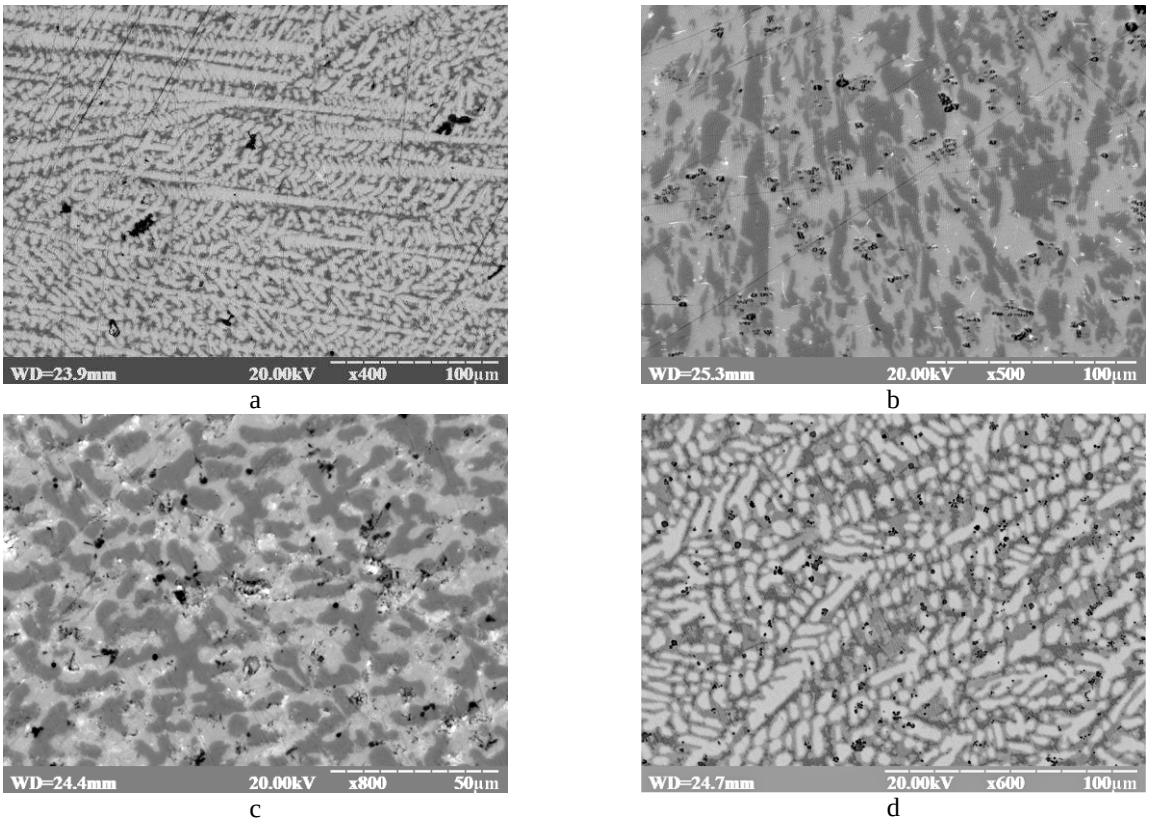

Fig. 2 Electron micrographs of selected alloys (numbered according to Table 1):
a) 6. $Sm_{45}Cu_{35}Sn_{20}$ – SmCuSn (light phase); Sm_5Sn_3 (gray phase); $SmCu_2$ (dark gray phase);
b) 9. $Sm_{23}Cu_{40}Sn_{37}$ – $Sm_3Cu_4Sn_4$ (light gray phase); $SmCu_2Sn_2$ (gray phase);
c) 12. $Sm_{30}Cu_{20}Sn_{50}$ – $Sm_3Cu_4Sn_4$ (gray phase); $SmSn_2$ (light gray phase);
d) 5. $Sm_{20}Cu_{60}Sn_{20}$ – $Sm_{1.9}Cu_{9.2}Sn_{2.8}$ (gray phase); SmCuSn (light gray phase); $SmCu_5Sn$ (dark phase).

Table 2 Crystallographic data for the ternary compounds in the Sm–Cu–Sn system at 870 K.

No. [a]	Compound	Structure type	Space group	Unit cell parameters, nm		
				a	*b*	*c*
1	$SmCu_5Sn$	$CeCu_5Au$	*Pnma*	0.8267(1)	0.50087(6)	1.0601(1)
2	$Sm_{1.9}Cu_{9.2}Sn_{2.8}$	related to $CeNi_5Sn$	$P6_3/mmc$	0.5044(3)	–	2.0428(9)
3	SmCuSn	NdPtSb	$P6_3mc$	0.4546(1)	–	0.7463(4)
4	$Sm_3Cu_4Sn_4$	$Gd_3Cu_4Ge_4$	*Immm*	1.4824(6)	0.6961(3)	0.4506(3)
5	$SmCu_2Sn_2$	$CaBe_2Ge_2$	*P4/nmm*	0.4402(2)	–	1.0948(8)

[a] The compound number corresponds to the number in the phase diagram (Fig. 1).

Gd-Yb, showed the formation of ternary phases at the composition $R_{15}Cu_{70}Sn_{15}$, which crystallized with $CeCu_5Au$- or $CeCu_6$-type structure [18-20], and $R_{1.9}Cu_{9.2}Sn_{2.8}$ compounds (found at the composition ~$R_{14}Cu_{66}Sn_{20}$, R = Y, Ce-Sm, Gd-Lu) with a hexagonal structure related to the $CeNi_5Sn$-type [12]. X-ray analysis of the samples in the Cu-rich corner of the Sm–Cu–Sn system showed the formation of the $SmCu_5Sn$ stannide with $CeCu_5Au$-type and the $Sm_{1.9}Cu_{9.2}Sn_{2.8}$ compound with a structure related to the $CeNi_5Sn$-type. During the present work, the crystal structure of the $SmCu_5Sn$ stannide was refined by X-ray powder diffraction. The crystal structure determination confirmed that the $SmCu_5Sn$ compound crystallizes with a $CeCu_5Au$-type structure (space group *Pnma*, a = 0.8267(1), b = 0.50087(6), c = 1.0601(1) nm), with the atomic parameters presented in Table 3.

Phase analysis of the $Sm_{15}Cu_{65}Sn_{20}$ samples annealed at 770 and 870 K clearly showed the presence of the hexagonal phase $Sm_{1.9}Cu_{9.2}Sn_{2.8}$ at both annealing temperatures. Taking into account the closeness of the composition of the $Sm_{1.9}Cu_{9.2}Sn_{2.8}$ compound ($Sm_{14}Cu_{66}Sn_{20}$) and the approximate composition $Sm_{15}Cu_{65}Sn_{20}$ reported in [6], we may state that the "$Sm_{15}Cu_{65}Sn_{20}$" phase corresponds to the $Sm_{1.9}Cu_{9.2}Sn_{2.8}$ stannide.

The ternary compound $Sm_2Cu_4Sn_5$ was not observed at 870 K. According to the X-ray diffraction and microprobe analyses, the sample belongs to the

three-phase field containing $SmCu_2Sn_2$, Cu_3Sn, and Sn. The $Sm_2Cu_4Sn_5$ compound was then studied by differential scanning calorimetry and the results confirmed the limited temperature range for this phase. The DSC curve measured in heating regime showed a thermal peak at about 811 K (Fig. 3), which can be associated with the decomposition of the $Sm_2Cu_4Sn_5$ phase, confirming the results of the phase composition of the samples near this composition at 870 K. We also performed DSC analysis on the isostructural compounds with Pr and Nd. Similarly to the Sm compound, the $Pr_2Cu_3Sn_6$ and $Nd_2Cu_3Sn_6$ stannides are characterized by limited temperature ranges of exisistence. The DSC curves of $Pr_2Cu_3Sn_6$ (heating regime) showed two thermal peaks at about 496 and 783 K (Fig. 4a), which can be associated with the formation of the phase and its subsequent decomposition, respectively. The DSC measurements of the $Nd_2Cu_3Sn_6$ compound also confirmed a limited temperature range for this phase, showing thermally induced transitions at 671 and 791 K, associated with formation and decomposition, respectively (Fig. 4b).

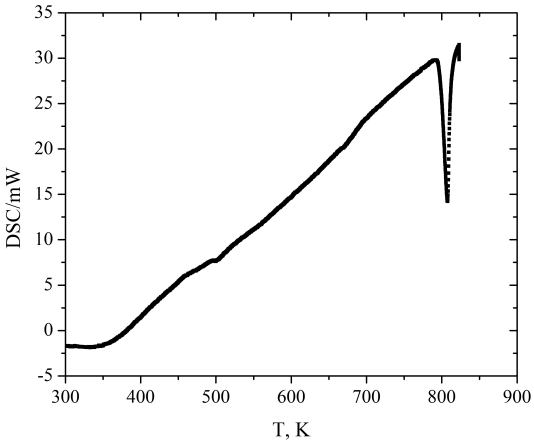

Fig. 3 DSC curve for $Sm_2Cu_4Sn_5$.

4. Final remarks

Comparing the present study of the Sm–Cu–Sn system at 870 K, and the investigation at 770 K reported in [6], the formation of five ternary compounds was observed at both temperatures: SmCuSn, $Sm_3Cu_4Sn_4$, $SmCu_5Sn$, $Sm_{1.9}Cu_{9.2}Sn_{2.8}$, and $SmCu_2Sn_2$,

Table 3 Atomic positional and isotropic displacement parameters for the $SmCu_5Sn$ compound (R_B = 0.042, R_p = 0.037, R_{wp} = 0.048).

Atom	Wyckoff position	*x*/*a*	*y*/*b*	*z*/*c*	$B_{iso}\cdot10^2$ (nm^2)
Sm	4*c*	0.2525(6)	¼	0.5622(4)	0.93(1)
Cu1	8*d*	0.0707(8)	0.4905(9)	0.3125(9)	1.24(2)
Cu2	4*c*	0.0610(8)	¼	0.0995(9)	1.68(2)
Cu3	4*c*	0.3176(9)	¼	0.2400(8)	1.35(3)
Cu4	4*c*	0.4206(9)	¼	0.0133(8)	1.03(3)
Sn	4*c*	0.1402(5)	¼	0.8575(4)	0.99(4)

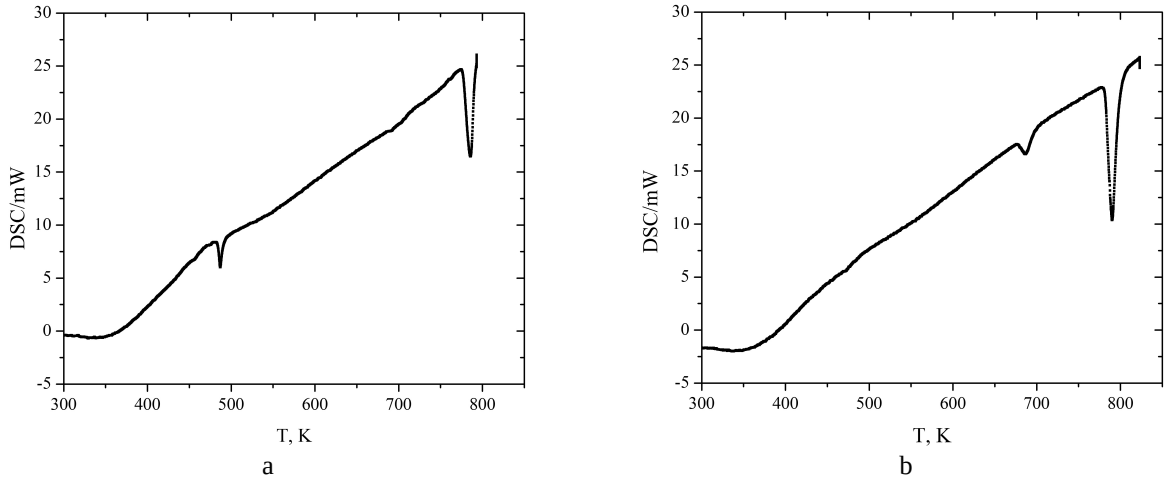

Fig. 4 DSC curves for $Pr_2Cu_3Sn_6$ (a) and $Nd_2Cu_3Sn_6$ (b).

i.e. all the compounds forming up to 40 at.% Sn are stable both at 770 and 870 K. On the contrary, the Sn-rich compound $Sm_2Cu_4Sn_5$ is characterized by a limited temperature range, similarly to other $R_2Cu_{4-x}Sn_{5+x}$ phases with Pr, Nd, Gd, Tb, and Dy. The results confirm the strong influence of temperature on the stability of *R*–Cu–Sn intermetallic compounds. Comparing the Sm–Cu–Sn system investigated here and other, previously studied *R*–Cu–Sn systems, a close analogy is observed regards the stoichiometry and crystal structure of most of the ternary compounds. The similar interactions of the elements in these systems lead to the formation of compounds *R*CuSn (NdPtSb-type), $R_3Cu_4Sn_4$ ($Gd_3Cu_4Ge_4$-type), $R_{1.9}Cu_{9.2}Sn_{2.8}$ (related to $CeNi_5Sn$-type), and RCu_5Sn ($CeCu_5Au$-type; not observed for Lu).

Acknowledgement

The work was supported by the Ministry of Education and Science of Ukraine (grant No. 0115U003257).

References

[1] P. Riani, D. Mazzone, G. Zanicchi, R. Marazza, R. Ferro, *Intermetallics* 5 (1997) 507-514.
[2] P. Riani, D. Mazzone, R. Marazza, G. Zanicchi, R. Ferro, *Intermetallics* 8 (2000) 259-266.
[3] P. Riani, M.L. Fornasini, R. Marazza, D. Mazzone, G. Zanicchi, R. Ferro, *Intermetallics* 7 (1999) 835-846.
[4] O.I. Bodak, V.V. Romaka, A.V. Tkachuk, L.P. Romaka, Yu.V. Stadnyk, *J. Alloys Compd.* 395 (2005) 113-116.
[5] I.V. Senkovska, Ya.S. Mudryk, L.P. Romaka, O.I. Bodak, *J. Alloys Compd.* 312 (2000) 124-129.
[6] G. Zanicchi, D. Mazzone, M.L. Fornasini, P. Riani, R. Marazza, R. Ferro, *Intermetallics* 7 (1999) 957-966.
[7] V. Romaka, Yu. Gorelenko, L. Romaka, *Visn. Lviv. Univ., Ser. Khim.* 49 (2008) 3-9.
[8] L. Romaka, V.V. Romaka, E.K. Hlil, D. Fruchart, *Chem. Met. Alloys* 2 (2009) 68-74.
[9] V.V. Romaka, D. Gignoux, L. Romaka, N. Skryabina, D. Fruchart, Yu. Stadnyk. *J. Alloys Compd.* 509 (2011) 5206-5210.
[10] T.B. Massalski, H.O. Okamoto, P.R. Subramanian, L. Kacprzak (Eds.), *Binary Alloy Phase Diagrams*, ASM, Metals Park, OH, USA, 1990.
[11] L. Romaka, V.V. Romaka, V. Davydov, *Chem. Met. Alloys* 2 (2008) 192-197.
[12] V.V. Romaka, D. Fruchart, R. Gladyshevskii, P. Rogl, N. Koblyuk, *J. Alloys Compd.* 460 (2008) 283-288.
[13] P. Villars, L.D. Calvert, *Pearson's Handbook of Crystallographic Data for Intermetallic Phases*, ASM, Metals Park, OH, USA, 1991.
[14] F. Weitzer, K. Hiebl, P. Rogl, *J. Solid State Chem.* 98 (1992) 291-300.
[15] M.L. Fornasini, P. Manfrinetti, A. Palenzona, S.K. Dhar, *Z. Naturforsch. B* 58 (2003) 521-527.
[16] L. Akselrud, Yu. Grin, *WinCSD: Software Package for Crystallographic Calculations* (Version 4), *J. Appl. Cryst.* 47 (2014) 803-805.
[17] T. Roisnel, J. Rodriguez-Carvajal, *WinPLOTR: a Windows Tool for Powder Diffraction Patterns Analysis*, *Mater. Sci. Forum* 378-381 (2001) 118-123.
[18] R.V. Skolozdra, L.P. Romaka, L.G. Akselrud, J. Pierre, *J. Alloys Compd*. 262-263 (1997) 346-349.
[19] Ya. Mudryk, O. Isnard, L. Romaka, D. Fruchart, *Solid State Commun.* 119 (2001) 423-427.
[20] M.L. Fornasini, R. Marazza, D. Mazzone, P. Riani, G. Zanicchi, *Z. Kristallogr.* 213 (1998) 108-111.